Modeling the draping of NCF composite preforms.

Muhammad-Ali Siddiqui, Colmar Wocke

The Dow Chemical Company, Bachtobelstrasse 3, CH-8810 Horgen, Switzerland

Abstract: *Non-Crimp Fabrics (NCF) are widely used textile reinforcements in fibre reinforced composite structures. The most important prediction from a draping analysis featuring preforms from these materials is their resulting fibre orientations; the orientations influence several other properties including fabric permeability and final component strength. The analysis is complicated by the influence of localized stitching patterns and their constraint on relative sliding of individual layers within a single ply during the draping process. The modeling procedure involves a process of material characterization valid for fabric preform materials and has been carried out using the Abaqus/Explicit finite element analysis code. The work is concerned with the development of such a predictive model using a rebar-approach in Abaqus. Biaxial and triaxial NCF are modeled using multiple shells. The anisotropic properties of the preform are naturally represented by the model. The details and capabilities of the model are discussed and qualitative comparisons are made with real preform shapes taken from NCF reinforcement on hemispherical dome forming experiments. The model has been used to compare predictions to the force vs. deflection results from single dome forming tests as well as the comparative ability to predict the location and severity of wrinkles. The current model demonstrates a high level of functionality allowing accurate prediction of yarn and stitch pattern movement. The adopted modeling technique, using separate shells works reasonably well, although it brings with it an increased requirement on computer resources.*

Keywords: *Abaqus, Preforms, Composite, Anisotropic.*

1. Introduction

Non-crimp fabrics (NCF) are aligned fabrics made from plies that are stitched together within a single ply with the stitching also looped as inter-ply stitching, to make up the full fabric. The reinforcement, say carbon fibre, is generally aligned within a plane, giving such NCF layers in principle better mechanical properties (Khan, 2010) than their woven counterparts provided “all other things are kept equal”. The stitching binds individual plies into a whole-layer assembly, so that the integrity of the fabric is fairly-well conserved; they do not fall apart so easily before they are placed into a mould and then infused with resin (Siddiqui, 2012). The same advantages at the layup stage, brings with it potential wrinkling issues when one wants to form or press such NCF into moulds when there is significant deformation required. International light weighting initiatives in the automotive industry have spurred a need for modeling the draping and deformation of NCF materials for complex geometries. Earlier work has been very successful in modelling this behaviour for woven-style fabrics (Wocke, 2014) based on the rebar approach in Abaqus.

Extending our existing capabilities for weaves to NCF-style fabrics is the focus of this paper. The process for arriving at a tuned finite element computational model, able to accurately describe local deformations for such NCF materials is discussed. Carrying the successful modelling technique for weaves, over to the NCF style of fabrics presented some initial difficulties. Since standard shell theory was not applicable, a modification of the earlier modelling approach was required. In the case of NCF, the individual plies needed to be modelled within a single shell in order to first capture the internal sliding degree-of-freedoms and then the additional stitching restraint needed to be modelled between the shells. A cursory literature survey (Mitchell, 2014), (Ji Seok, 2007) shows that the approach of modelling NCF using separate shells is common in purpose-written software (Willems, 2006). The process of going from a well-working single-shell modelling technique for the woven fabrics to that of modelling the NCF materials was not as smooth as initially thought and presented many challenges.

2. Experimental testing of NCF materials

The naming convention related to NCF material, that we have adopted for analysis purposes, is:

> "In general, an NCF ***layer*** is composed of individual ***plies*** of fibre rovings ***stitched*** together. A ***layer*** of NCF is an assembly of ***stitched plies***."

For example, a single biaxial +/-45 NCF is an entity named "layer" composed of two unidirectional "plies" with fibre rovings at +45 and -45 respectively. These plies are held together to act as an individual layer via stitches; a laminate of fabrics is composed of a number of layers.

2.1 Layer characterization

In developing testing protocols, we relied on a combination of brainstorming/technical evaluation sessions as well as a literature study (Kreissl, 2013), (Khan, 2010) to identify the test cases. In order to provide basic characterization, we carried-out two bias-extension tests for biaxial +/-45 NCF fabrics. The dimensions of the strip for the samples are 240 mm long by 120 mm wide; this ratio of length to width results in three characteristic deformation zones during the test, most easily seen for cases where there is appreciable internal fibre rearrangement. In the first test, the stitches were aligned to the loading direction, while in the second test the stitching ran perpendicular to the pull as shown in Figure 1.

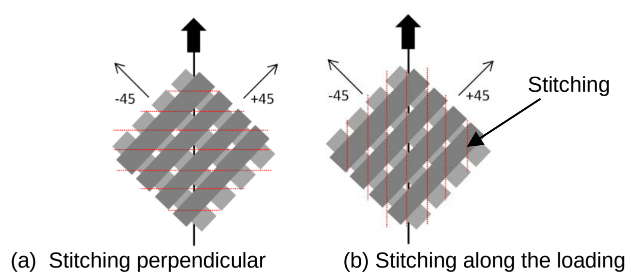

Figure 1. Unit cell of sample of +/- 45 NCF for experimental bias extension tests.

Results from the experimental tests are shown in Figures 2 and 3. For stitches along the loading direction, the load is able to be carried primarily by the carbon fibres with some small non-linear tightening, due to internal friction, of the stitches during deformation; cf. (Wocke, 2014) for an exposition of how the frictional resistance is generated inside such a layer.

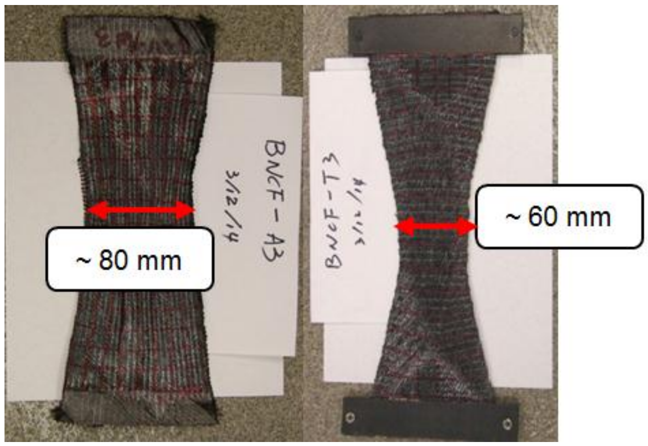

(a) Stitching running along the pull (b) Stitching running perpendicular.

Figure 2. Graphic of experimental deformation of bias test for NCF.

With the stitching running perpendicular to the pull direction, there was relative opening of the stitching and reorientation of the fibre tows i.e. the resistance is almost all due to internal frictional restraint between tows. Hence, the response on the force-displacement curve yielded very low values, by comparison to the case in Figure2a – it is essentially all frictional.

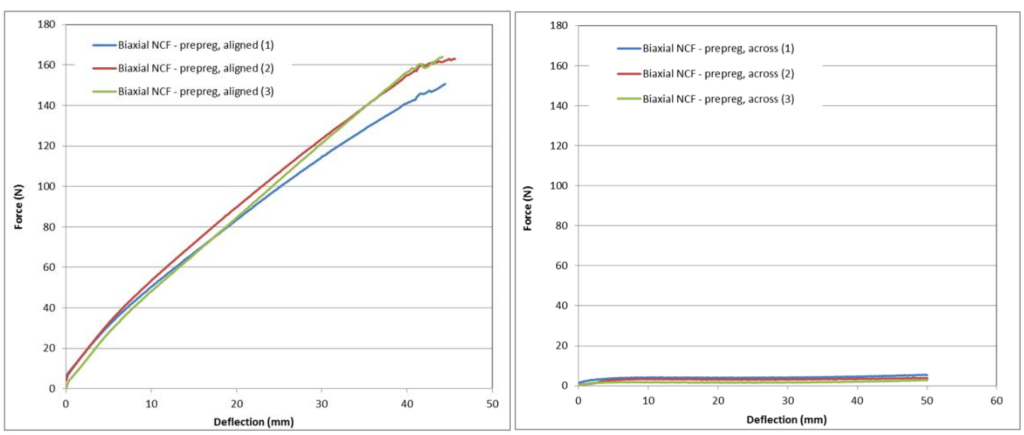

(a) Stitching running along the pull (b) Stitching running perpendicular.

Figure 3. Force-displacement response of the fabric.

The distinct deformation zones in the fabric which is a feature related to bias-extension tests can also be discerned with the naked eye during testing. Particularly, for the case when the stitches are running perpendicular to the pull direction, a central diamond and triangular areas at the top and bottom of the fabric sample developed, in agreement with the expected, clear delineation of zones. This can be quite clearly seen in Figure 2b.

3. Modeling the behaviour and calibrating

In order to model the in-plane behaviour of an NCF layer, we need at a minimum, a description of a ply response. The stitching within the ply modifies this behaviour in the sense that it introduces an additional orthotropy in the response, which also needs to be accommodated. To model a fabric, we need to include a representation of the response/constraints provided by the stitching between layers. The calibration has been performed on an FEM model representative of the bias test; basically a strip held at one end and pulled at the other. To obtain the analysis data for comparison to the test crosshead data easily from the Abaqus model, two single nodes were tied via respective `*MPC` keywords to the edges of the shell; the one node was held fixed; the other was given a prescribed displacement.

3.1 Single-shell approach

The single-shell approach is similar to in our previous work on weaves already presented (Wocke, 2014) where the response of the fibres is modeled using a shell section reinforced with internal rebars aligned to represent the fibre tows.
In Table 1 details regarding the architecture and material properties of the fabric are included, in order to be able to specify the rebar properties.

Table 1. Summary of architecture & material properties of biaxial +/-45 NCF.

Dry Areal Weight (gsm)	600 (300/300)
Strength	4200 MPa
Elastic Modulus	240 GPa
Fibre count	24k
Fibre diameter	7e-6 m

As an illustration, using the single-shell approach, consider the case of the stitches running perpendicular to the loading direction. The simulation results from the model for this case are shown in Figure 4. When compared to the experimental tests, the FE results over-estimated the inward movement of the fabric. As shown in Figure 4, the minimum width at the centre from the experimental results was approximately 60 mm while the FEM predicted resulted were ca. 20 mm. Hence, a much narrower hour-glass shape is predicted. This is attributed the kinematics of deformation of a single-shell where the effects of the very high Poisson’s ratio, as a consequence of the +/-45 rebar, are predominant since the shell is so well-connected internally.

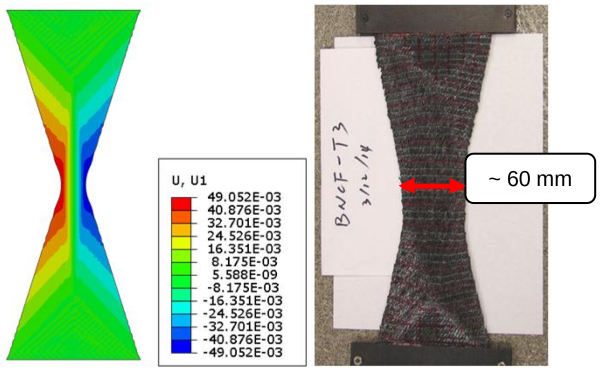

Figure 4. Comparison of the FEM results from bias test simulation for Biaxial +/-45 NCF for stitching running perpendicular to the pull with experiment.

The comparison of the predicted reaction force vs. displacement results to the experimental ones is presented in Figure 5.

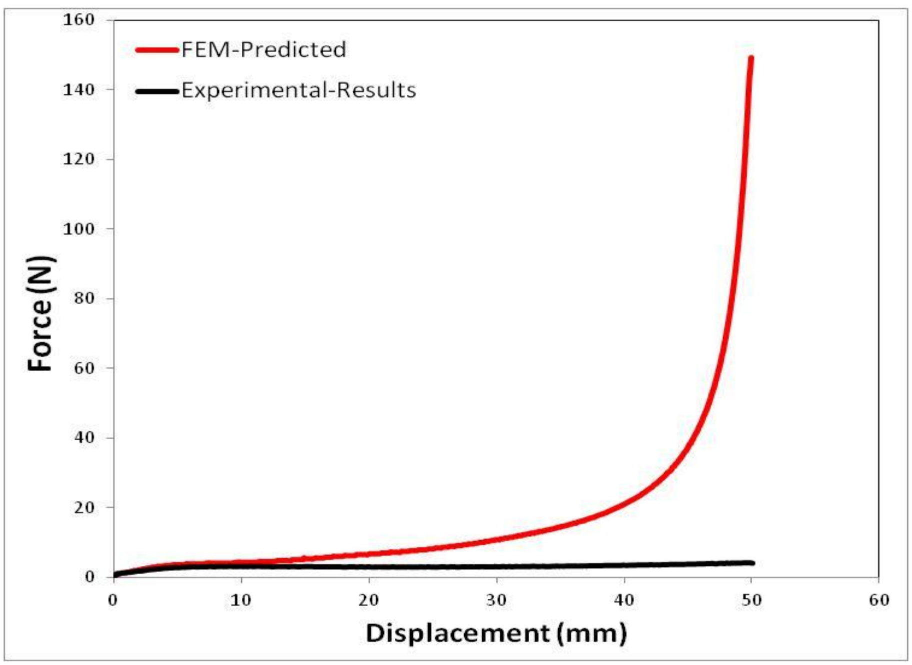

Figure 5. Comparison of force vs. displacement results for single shell bias test.

3.2 Kinematics of deformation of NCF

The deformation mechanism of a single layer of NCF material is governed by the relative motion of the fabric plies. These plies are stitched together, yet still can ***slide*** relative to one another during deformation. Nevertheless, the deformation mechanism of NCF is not based on interlocking of warp and weft tows as is the case in the woven fabrics (Wocke, 2014). From the general shell theory, independent relative sliding of rebars cannot be captured while defining the set of rebars layers with different orientations within a single-shell as shown in Figure 6:

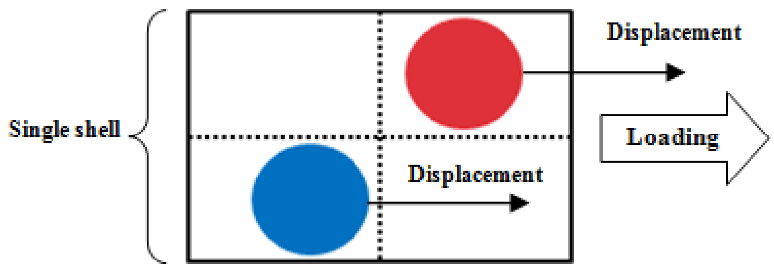

Figure 6. Kinematics of deformation of single shell with rebars.

3.3 Characterization of base-shell using pseudo UD response

In principle, a single layer of NCF consists of two plies (or two half layers) of fabric, suitably-oriented. Within each ply, there is interply friction as the fibre tows slide against/past one another as has been illustrated in Figure 6 and between these plies there is more friction, making up the full internal frictional/resistance of the whole layer. In addition to the friction, there's the internal restraining effect of the stitching which almost invariably increases as a result of severe deformation. This restraining effect acts within a ply as well as between plies when these are assembled into a layer and eventually into a fabric.

A workable technique we've adopted, after some numerical experimentation, is to tune out the base shell w.r.t. a half shell or ***one ply***. This allows us to define the interply behaviour, using the general procedure for tuning out the bias-extension test behaviour; the details of this are in our earlier paper (Wocke, 2014). This tuned model then serves as the basis for describing the +/-45 NCF biaxial and a generic triaxial +60/-60/0 fabrics. When this is extended to the full layer, then we only need to define the separate shells with restraint ***between*** them. The last value of restraint needs to be tuned out from the experimental feedback from the single dome forming experiments. In essence, our approach separates the contribution due to interply effects from those between plies – the interply response has the orthotropic restraint effects captured by the ***ghost layer*** description defined within the shell section.

The predicted reaction force vs. displacement results for the pseudo UD response for the two experimental cases are presented in Figure 7.

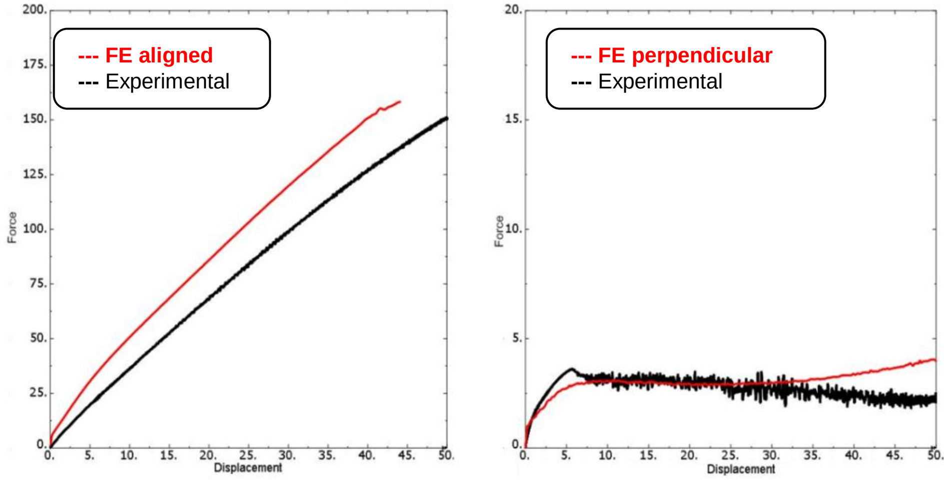

(a) stitching along the loading (b) stitching running perpendicular

Figure 7. Comparison of Force vs. displacement-Predicted results for bias test for pseudo UD shell.

3.4 Multiple-shell approach for NCF

The details of the computational model development for multiple shell approach is not disclosed in this paper– this is proprietary to DOW, but rather we focused to illustrate some of the analysis possibilities that are enabled by such a model.

In the multiple shell approach, each shell section represents an individual ply of the layer and their directions. For the multiple-shell approach, the summary of steps taken for material parameterization is as follows:

1. Model each ply's interaction behaviour of the NCF layer as a ***separate*** shell mesh.
2. In each shell in the ***SHELL SECTION, COMPOSITE** definition, define rebar orientation according to fibre tow directions of the ply.
3. Use ***POTENTIAL** to account for the reduction/alteration of stitching contribution and orientation within the ***ghost layer.***
4. Define individual thicknesses to each ply i.e. ***layer thickness ÷ no. of shell meshes.***
5. Define relative sliding definitions between shells using:
    i. Use ***FRICTION** between each ply of the layer to control relative sliding *and/or*
    ii. Use ***BOND** to control relative sliding *and/or*
    iii. Define *trusses* to connect nodes of individual shell sections to control relative sliding *and/or*
    iv. Use **COHESIVE CONTACT INTERACTION BEHAVIOUR** to control sliding of plies.
6. Run analyses for pulling experiment & correlate results.

When constraining the shells together, we investigated the use of different options available in Abaqus. A summary of our findings is given below:

1. ***BOND**: *this option is intended for modeling local spot welds between adjacent nodes. However, this can only be used in single cpu analyses. Using* ***BOND** *will not be viable due to extremely long computation times.*
2. **COHESIVE CONTACT BEHAVIOR**: *this option is based on modeling surface-to-surface contact between adjacent faces.*
3. ***FRICTION** *used to define the restraint force between the shell surfaces of the plies, can be used in multiple cpus analyses.*

Defining coefficient of friction and cohesive contact interaction definition are found to be the best options as far as computational resource cost are concerned.

The deformed shape comparison results for the bias extension test for biaxial +/- 45 NCF using multiple shells approach, with stitching running along the loading direction is shown in Figure 8. The visual agreement shows very good correlation, as is the case for the force-deflection results, presented in Figure 9.

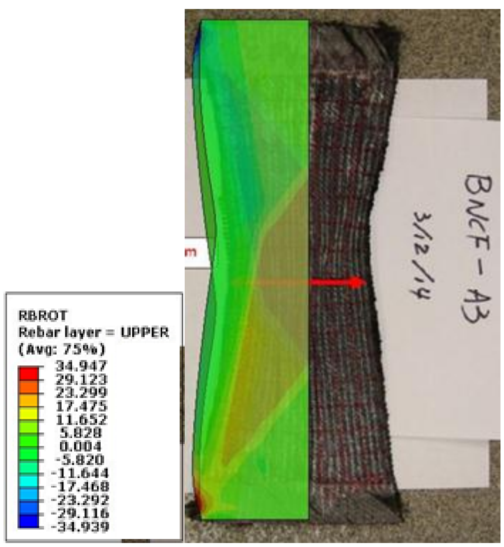

Figure 8. Comparison of deformed shape & rotation of fabric for biaxial NCF +/- 45 along the stitching bias extension tests.

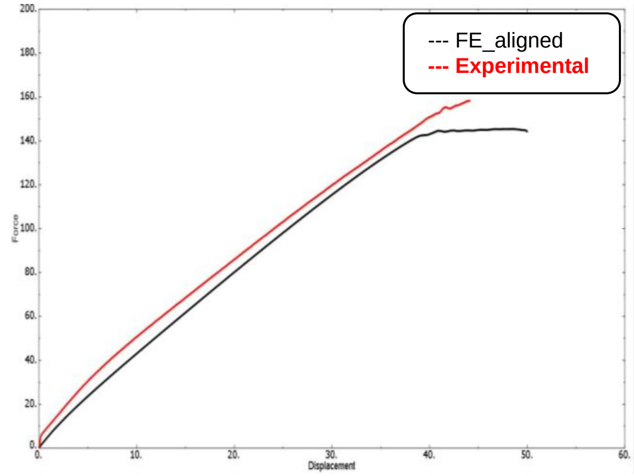

Figure 9. Comparison of predicted force displacement with experimental results for biaxial NCF +/- 45 along the stitching bias extension tests.

Carrying out the simulation for the bias extension test case, where the stitching runs perpendicular to the loading only requires an orientation change of the ***ghost*** material in the input file, since the plies lie at +/- 45. In our case, the ghost is hence rotated by 90^{o}, making an equivalent change in the `*POTENTIAL` keyword; for the general case, one would perform this via an `*ORIENTATION` keyword. The experimental test suggests that the stitching may open up, which is not possible to capture with a smeared shell model. Very little locking of the fabric is observed during the loading. The results obtained in the multiple-shell bias extension test, for biaxial +/- 45 NCF, when the stitching is running perpendicular to the loading direction are shown in Figure 10, with the force-deflection results presented in Figure 11:

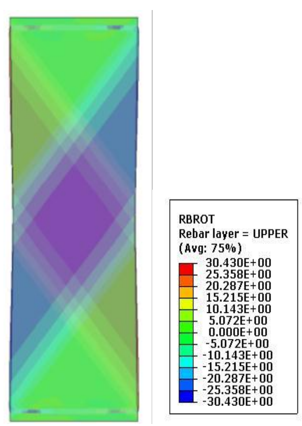

Figure 10. Comparison of deformed shape & rotation of fabric for biaxial NCF +/- 45 across the stitching bias extension tests.

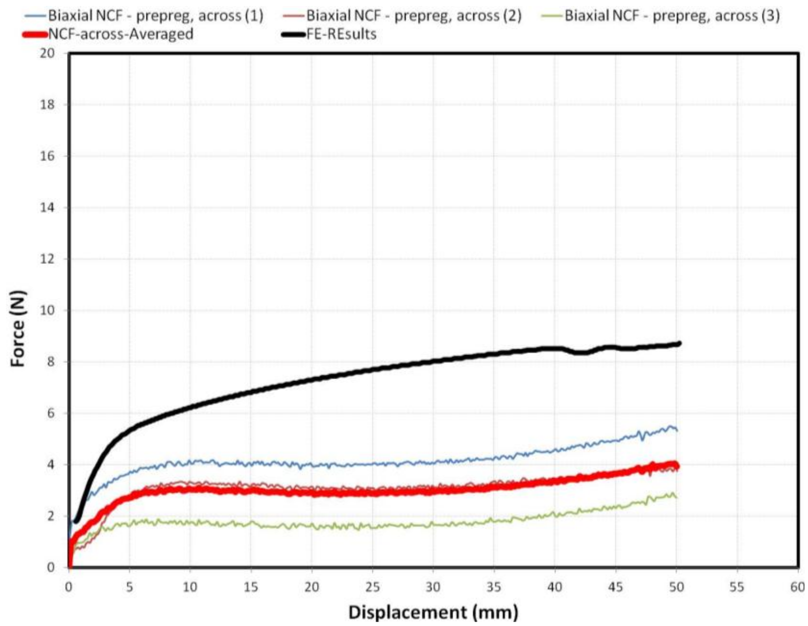

Figure 11. Comparison of predicted force displacement with experimental results for biaxial NCF +/- 45 across the stitching bias extension tests.

An over-estimation of the force-displacement response is observed from the predicted results; fine tuning of the data on the ***POTENTIAL** keyword did not provide enough possibility (Simulia, 2013) to reduce the orthogonal response contribution of the ghost layer representing the stitching. The magnitude of force along this direction is very small and global errors due to the overall distribution of the force would be small in comparison to the forces introduced from the other direction. Further fine tuning of the process parameters may help reduce this error and additional work in this regard is still under progress.

4. Implementation of NCF computational model to hemisphere draping

4.1 FEM description of inverse draping test

The model represents a 350mm square sheet of preform fabric, being pushed into a die using a round-nosed punch. The fabric is laid flat onto the flat peripheral surface of the die (base) and held in place by a blank-holder (binder). The pertinent geometric dimensions for the analytical rigid surfaces in the problem are shown in Figure 12 (Jauffrès, 2010). The binding force is held constant, once contact has been established between preform and the die periphery. Analytical rigid surfaces represent the rigid surfaces, with the preform modelled using **S4R** elements. Friction is constant, using 0.3 as the friction coefficient (static friction only).

The FEM analysis was carried out using the multiple-shell approach and the material parameters as discussed in the previous section; the binding force is 650N in the case of biaxial NCF +/- 45 and 3100N, in the case of triaxial +60/-60/0 NCF.

The analysis is performed in 3 steps, similar to what was done in Problem 1.3.3 in the Abaqus Example Problems Manual (Simulia, 2013) and in our previous work on weaves (Wocke, 2014):

Step 1 – Establish contact, using softened exponential contact to avoid “numerical chattering”.
Step 2 – Apply the preload onto the binder, via its reference node.
Step 3 – Move the punch reference node by the required displacement.

The punch is moved 60mm downwards in a `*DYNAMIC, EXPLICIT` step in Abaqus/Explicit.

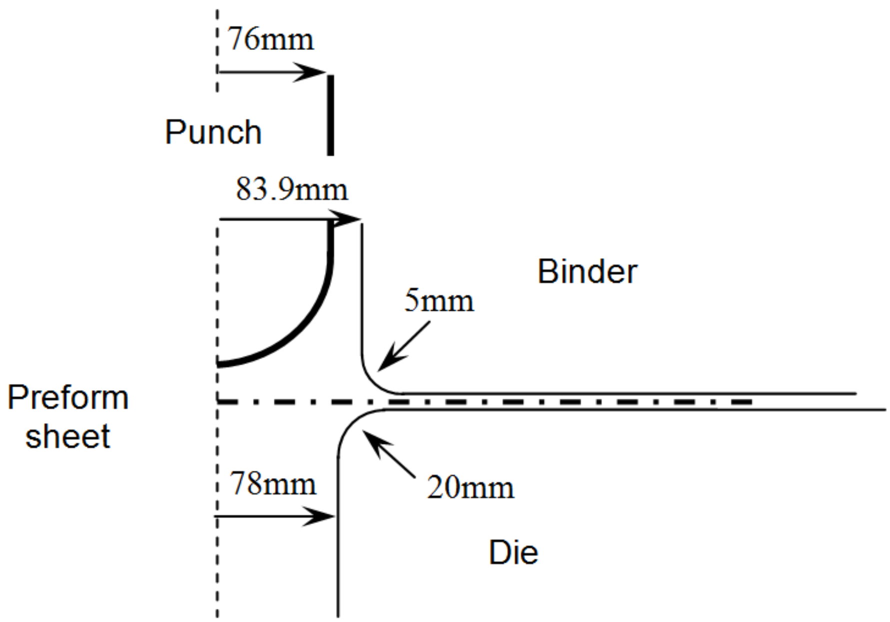

Figure 12. Geometric details of the surfaces for hemisphere draping.

4.2 Biaxial +/-45 NCF test

In this experiment, the NCF layer of two plies has fibres of the top ply aligned with the global x- and bottom ply with y-directions, respectively. The stitching is aligned -45 degree to the horizontal plane which is modelled using a ghost layer within the composite shell section. The predicted deformed shape is shown in Figure 13. The predicted results show excellent visual agreement with experimental results; the wrinkling patterns and their general locations are well captured, with well-controlled sliding between layers.

Figure 13. Predicted deformed shape of biaxial +/-45 NCF (stitching reorientation is displayed with white-lines in FEM results).

4.3 Triaxial +60/-60/0 NCF test

The triaxial fabric used in this experiment consists of 3 plies, oriented at +60/-60/0; the stitching is along the horizontal x-axis of the tool surface. The deformed shape, together with the location of the dominant wrinkles, is shown in Figure 14, shows good visual agreement with experimental results. As was the case with the biaxial fabric, the relative sliding of the individual plies is well-controlled, without any disturbing relative movement of the three shells over each other.

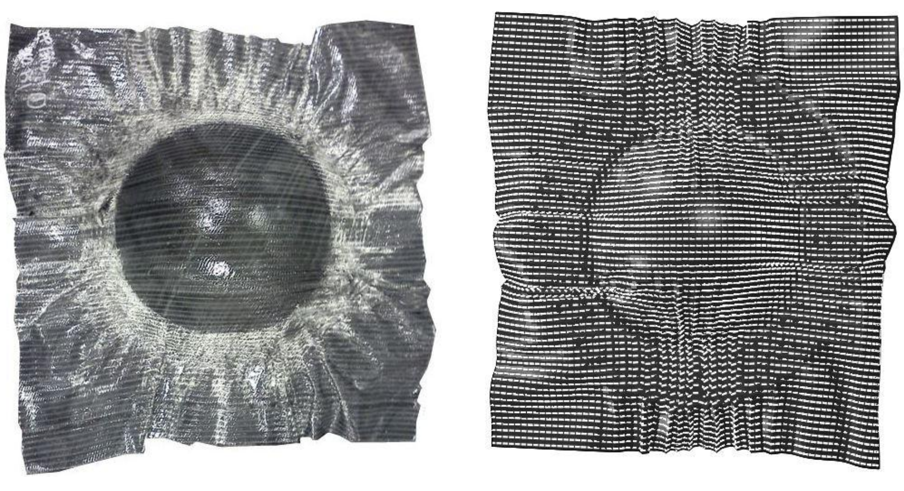

Figure 14. Predicted deformed shape with experimental results for triaxial +60/-60/0 NCF (stitching reorientation is displayed with white-lines in FEM results).

Even though the detailed internal deformation mechanism of triaxial NCF is different from the woven fabric, the general shape of the force-displacement response of the triaxial NCF fabric during hemisphere test is similar to that of woven fabrics. The predicted reaction force of the punch is overly flexible at the beginning and then becomes overly stiff as the punch continues past 60 mm of displacement, as shown in Figure 15. The stiffer response at ca. 60 mm is attributed to the interlocking of the stitching and the pressure dependent increasing friction restraint between the plies; the resolution of this effect is left for future work.

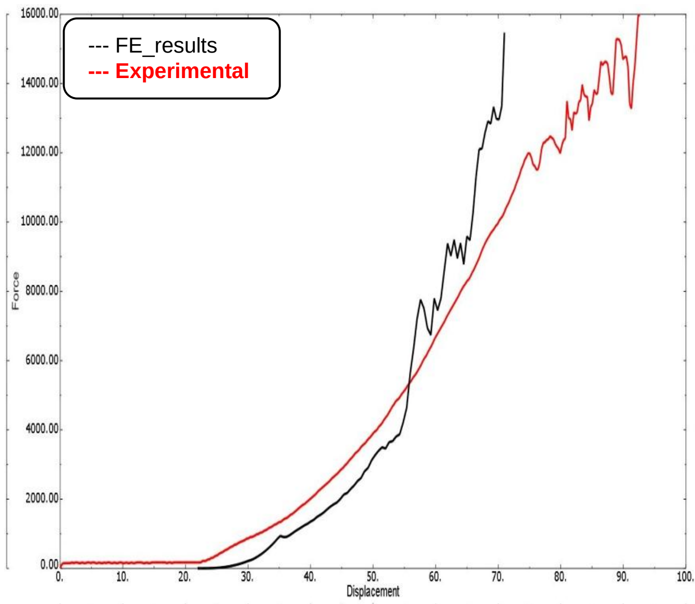

Figure 15. Comparison of predicted force-displacement with experimental results for triaxial NCF.

5. Conclusions & Recommendations

Our approach for modelling the NCF as suitably-oriented rebars within separate shells with constraints between them, using the existing modelling capabilities within Abaqus has been demonstrated. The approach we have used for the material parameterization is to tune the response of a single ply through its rebar contribution and a suitable material model for the internal friction between tows, supplemented by a ghost stitching layer and adjustments for orthogonality using the **`*POTENTIAL`** keyword. Once acceptable numerical agreement is obtained for a single ply, it may be combined with others into a single shell. Single shells, in turn are constrained to slide/move over one another in a fabric, using cohesive contact behaviour. The predictive modeling approach was demonstrated in the hemisphere draping of NCF type materials; we were able to predict fibre rearrangement and the general occurrence of wrinkling. The relative sliding of the individual plies was controlled and we did not notice any large relative movement of the two shells over each other; the cohesive contact behaviour defined in the analyses was able to control the movement of the elements with acceptable agreement to the experimental results.

Our future work will focus on implementation of this approach to more complex shapes and also carry out experimental correlation for predicted fibre rotations with experiments.

Modeling the NCF fabric using separate shells brings with it an increased requirement on computer resources. Currently, we have no alternative way for modelling these, except by writing custom routines to better describe the NCF properties.

6. Acknowledgements

Acknowledgements go to Dr. Liangkai Ma for analyses on hemisphere draping & Mr. Jay Tudor from Dow for supplying the required material and the experimental test data during the computational material model development.

7. References

1. Muhammad Aurangzeb Khan, "Numerical & experimental forming analyses of textile composite reinforcements based on a hypoelastic behaviour", PhD thesis for Ecole Doctorale des Sciences de l'ingénieur de Lyon, France 2009-2010.
2. Siddiqui, M. Ali, "High Pressure RTM Process modeling of Carbon Fibre Composites with Ultra-Fast-Cure resins", Kunststoffe + SIMULATION 2012, 23 & 24 April 2012, München, Germany.
3. Wocke, C. & Siddiqui M.A. "Using the existing capability in Abaqus to model the draping & consolidation of composite preforms", Proceedings of 2014 SIMULIA Community Conference.
4. Mitchell Cynthia J., Sherwood James A., Dangora Lisa M.,and Gorczyca Jennifer L. , "Using Abaqus/CAE and User-Defined Material Subroutines to Predict the Deformations of a Stitched Triaxial Fabric during Forming Processes", Proceedings of 2014 SIMULIA Community Conference.
5. Ji Seok Lee, Seok Jin Hong, Woong-Ryeol Yu, Tae Jin Kang, "The effect of blank holder force on the stamp forming behavior of non-crimp fabric with a chain stitch", Composites Science and Technology 67 (2007) 357–366.
6. Willems A., Lomov S. V., Vandepitte D. and Verpoest I., "Double dome forming simulation of woven textile composites", 7th International Conference ESAFORM 2006, Glasgow, UK, April 26-28,2006, S747-S750.
7. Kreissl S., Senner T., Lipp A., Meinhardt J., "Umformsimulation von Faserverstarkten Kunststoffen", LS-DYNA Anwenderforum, Filderstadt, 25th September 2013.

8. Khan M.A., Mabrouki T., Gauthier S., Vidal-Salle E., Boisse P., “Preforming simulation of reinforcements of woven composites approach within a commercial code”, LaMCoS, INSA-Lyon, CNRS UMR5259, F69621, France, URL: www.insa-lyon.fr

9. Abaqus 6.13, Documentation Collection, Abaqus Example Problems, Keywords & Theory Manuals, Simulia.

10. Jauffrès, David, Sherwood, James A., Morris, Corey D., Chen Julie, “Discrete mesoscopic modeling for the simulation of woven-fabric reinforcement forming”, International Journal of Material Forming (2010) 3 (Suppl. 2):S1205–S1216.